



HAL
open science

Metal-containing PAS/GAF domains in bacterial sensors

Romain Pardoux, Alain Dolla, Corinne Aubert

► **To cite this version:**

Romain Pardoux, Alain Dolla, Corinne Aubert. Metal-containing PAS/GAF domains in bacterial sensors. *Coordination Chemistry Reviews*, 2021, 442, pp.214000. 10.1016/j.ccr.2021.214000 . hal-03249747

HAL Id: hal-03249747

<https://hal.science/hal-03249747>

Submitted on 4 Jun 2021

HAL is a multi-disciplinary open access archive for the deposit and dissemination of scientific research documents, whether they are published or not. The documents may come from teaching and research institutions in France or abroad, or from public or private research centers.

L'archive ouverte pluridisciplinaire **HAL**, est destinée au dépôt et à la diffusion de documents scientifiques de niveau recherche, publiés ou non, émanant des établissements d'enseignement et de recherche français ou étrangers, des laboratoires publics ou privés.

Metal-containing PAS/GAF domains in bacterial sensors

Romain Pardoux^a, Alain Dolla^b and Corinne Aubert^{a#}

a. Aix Marseille Univ, CNRS, LCB, Marseille, France

b. Aix Marseille Univ, Toulon Univ, CNRS, IRD, MIO, Marseille, France

[#]To whom correspondence should be sent: *E-mail*: aubert@imm.cnrs.fr;

Keywords: Metals, PAS domains, GAF domains, Sensors, Two-component systems, σ^{54} -Dependent activators.

Highlights

- PAS/GAF domains bind disparate metal cofactors
- Metal can be the signal sensed by the PAS/GAF sensor
- O₂ and redox potential are the favorite signaling stimuli of metal-binding PAS/GAF
- Metal-binding induces conformational changes that modulate the effector activity

Abstract

PAS and related GAF are ubiquitous and highly versatile sensing domains that associate a range of signaling effectors. Each year, new bacterial PAS and GAF domains are characterized but genomes analysis suggests this list is far from complete.

This review aims to synthesize the current state of knowledge on the structure and activity of metal-binding PAS/GAF domain proteins. PAS/GAF domains can bind disparate metal cofactors with very precise coordination and high specificity concomitant with their extensive sequence diversity. Bound-metal can directly be the signal or can mediate signal detection such as gases or redox variation. Metal-containing PAS/GAF input modules are mainly associated to histidine kinases of two-component signaling systems and σ^{54} -dependent transcription factors. In both cases, metal-binding induces conformational changes that modulate the effector activity.

It appears that metal-containing PAS/GAF domains, as other PAS/GAF domains, offer great possibilities for coupling a broad range of ligand binding to various cellular responses and it is very likely that they have not yet revealed all their secrets.

33	Contents
34	1. Introduction
35	2. Structural basis of metal-binding in the PAS and GAF domain family proteins
36	2.1 Divalent metal cation-binding PAS/GAF domain
37	2.2 Heme-binding PAS domain
38	2.3 Fe-S cluster -containing PAS domains
39	3. Activity, signal sensing and signal transduction of metal-containing PAS/GAF
40	bacterial sensors
41	3.1. Two-component systems with input metallic PAS/GAF domains
42	3.1.1 Repression of TCS metal-containing PAS/GAF bacterial sensors by O ₂
43	3.1.2 Activation of TCS metal-containing PAS/GAF bacterial sensors by O ₂
44	3.1.3 Repression of TCS-containing PAS/GAF bacterial sensors by direct metal-
45	sensing
46	3.2 σ^{54} -Dependent activators with input metallic PAS/GAF domains
47	4. Conclusion
48	References
49	
50	

51 1. Introduction

52

53 To survive, living organisms must adapt to new environments or to changes in their current
54 environment. Bacteria actively sense and adapt to environmental cues through sensory and
55 signal transduction systems. Per-ARNT-Sim (PAS) and cGMP-specific phosphodiesterases,
56 adenylyl cyclases and FhlA (GAF) domains are common components of signal transduction
57 systems serving as universal signal sensors and interaction hubs [1-4]. Both PAS and GAF
58 domains are composed of ~ 110 amino acids with limited primary sequence homology but share
59 a remarkably conserved core structure [3-6]. Although PAS and GAF domains are distinguished
60 in the sequence-based annotations in the Pfam database [5], they are linked by evolution and
61 are structurally and functionally related [1,3,6]. Hence, they are considered together in this
62 review. PAS/GAF occur in all living organisms but are most highly represented among
63 prokaryotic genomes, with 90% of PAS domains identified in Eubacteria [2,7]. For example,
64 the deltaproteobacteria *Desulfovibrio* contains the largest number of PAS domain proteins (141)
65 found in a genome [7]. PAS/GAF-containing proteins can contain both PAS and GAF domains
66 or several PAS/GAF domains but are commonly associated with a wide range of enzymatic and
67 non-enzymatic functions [2,4]. PAS/GAF proteins play roles as receptors, signal transduction
68 mediators and transcription factors [4]. In bacteria and archaea, PAS/GAF clusters are mostly
69 involved in two-component systems such as histidine kinases, but they have been identified in
70 other proteins, such as serine/threonine kinases, guanylate cyclases, phosphodiesterases, ion
71 channels, chemotaxis proteins and transcription factors [3-5].

72 PAS/GAF domains usually serve as versatile sensors and interaction modules in signal
73 transduction proteins. These domains mainly exert their physiological roles without cofactors
74 but some of them have been shown to bind cofactors to regulate the activity of certain effector
75 domains [2,3,8]. Hence, cofactors such as hemes, flavins, di- and tricarboxylic acids, amino
76 acids, divalent metal cations, coumaric acid, fatty acids, non-heme iron and Fe-S clusters can
77 be found in PAS/GAF domains [2]. These cofactors, either covalently or not covalently bound
78 to the sensory module, can emit a signal to which the proteins directly respond or mediate signal
79 detection. In all cases, the signal is propagated to the effector domain by mechanisms and
80 strategies that diverge according to the PAS/GAF module [2,3,8].

81 Predictions of the functions of PAS/GAF domain proteins based on sequence and signal
82 transduction information remain challenging. Comparison of structurally and functionally
83 characterized PAS and GAF domain-containing proteins known to bind ligands will help to

84 identify the functions/activities of PAS/GAF proteins that have not yet been characterized.
85 Henry and Crosson in 2011 [2] and Uden et al in 2013 [8] provided overviews of the PAS/GAF
86 signaling protein diversity in prokaryotes. This review aims to synthesize the current state of
87 knowledge on the structures and activities of these proteins, focusing on metal-binding
88 PAS/GAF domains associated with two-component signal transduction systems (TCS) and σ^{54} -
89 dependent transcriptional regulators proteins (Figure 1).

90

91 **2. Structural basis of metal-binding in the PAS and GAF domain family** 92 **proteins**

93 The PAS domain is composed of five β -strands and four α -helices organized in four main
94 structural elements: the PAS core, the β -scaffold, the helical connector and the N-terminal cap
95 (Figure 2A) [4]. Despite the possibility of an additional antiparallel β -sheet in the GAF domain,
96 the GAF core itself is small and folds similar to the PAS core [3]. By way of example,
97 Photoactive Yellow Protein, which entirely consists of a single PAS domain, is closely
98 superimposable with the GAF domain of the YGK9 protein over a region that comprises the
99 beta-sheet and the irregular layer (Figure 2B) [2].

100 PAS/GAF domains can bind a large variety of metallic ligands, including metal-containing
101 cofactors such as heme, Fe-S clusters, and divalent metal cations, which contribute to the
102 determination of the input signal [2].

103

104 **2.1 Divalent metal cation-binding PAS/GAF domain**

105 Non-heme iron is found in the GAF domain of NorR, a bacterial enhancer-binding protein
106 (bEBP) of the AAA⁺ class of proteins that activates the σ^{54} -dependent transcription of *norVW*
107 in response to NO [9]. EPR spectroscopy has shown that the N-terminal GAF domain of NorR
108 contains a non-heme iron center that binds NO to form a high-spin $\{\text{Fe}(\text{NO})\}^7$ ($S=3/2$) complex
109 [10]. A model with the hexa-coordination of Fe involving three aspartates, one of which being
110 bidentate, one cysteine and one arginine residue, has been proposed; the arginine residue is
111 displaced to form the mononitrosyl iron complex (Figure 3) [11].

112 Other cations, such as Mg^{2+} , Ca^{2+} or Zn^{2+} , are cofactors of PAS domain-containing proteins.
113 Crystal structures of the *Escherichia coli* and *Salmonella typhimurium* periplasmic sensor
114 domains of PhoQ reveal that these structures fold into a PAS domain but with some striking
115 differences, as the insertion of α -helices creates a large negatively charged area that is partially
116 involved in the binding of divalent cations such as Mg^{2+} or Ca^{2+} (Figure 4) [12,13]. In the

117 presence of Mg^{2+}/Ca^{2+} , a bridge between the negatively charged PhoQ surface and negatively
118 charged bacterial phospholipids can form; upon release of the divalent cations from the PhoQ
119 sensor domain, repulsion between the negatively charged PhoQ surface and the membrane can
120 result in a change in their orientation relative to the membrane. This change corresponds to the
121 initial event in transition from a repressed to an active PhoQ conformation [12]. In the PAS
122 domain of the phosphoglycerate kinase in *Leishmania major*, it has been shown that a single
123 histidine residue is essential for Mg^{2+} binding in the absence of substrate; repression of PGK
124 activity is performed by the Mg^{2+} cation bridge formed between the PAS and PGK domains
125 [14]. Recently, the structure of the PAS domain of the WalK sensor from *Staphylococcus*
126 *aureus* was resolved [15]. The structure revealed the presence of a Zn^{2+} ion bound to the surface
127 of the PAS domain (Figure 5A). This feature enables Zn^{2+} in the surrounding solvent to access
128 the binding site. The Zn^{2+} ion adopts a slightly distorted tetrahedral coordination geometry by
129 binding to two N δ 1 atoms from two histidine residues, one O δ 1 atom from an aspartate residue
130 and one O ϵ 3 atom from a glutamate residue (Figure 5B). Structural and molecular dynamics
131 simulations of WalK suggested that Zn^{2+} binding directly influences the relative positioning of
132 the cytoplasmic PAS and CAT domains; upon Zn^{2+} binding the dihedral angle between the two
133 domains varied from 136° to 175° and the average distance between the upper and lower helices
134 of the cytoplasmic domain decreased from 21.6 Å to 12.3Å (Figure 5C, [15]). These large
135 conformational changes, induced by Zn^{2+} binding, would regulate the activity of the protein
136 [15].

137

138 2.2 Heme-binding PAS domain

139 Heme cofactor is found in several classes of PAS/GAF domain-containing proteins, including
140 FixL, DosP, Aer2, DosS/DevS [16-19]. Among the heme-containing PAS domains, FixL has
141 been the most extensively studied. The three-dimensional structure of the FixL PAS domain in
142 *Rhizobium meliloti* and *Bradyrhizobium japonicum* revealed that the heme iron is
143 pentacoordinated by a histidine residue, with no other ligand coordinating the sixth position
144 (Figure 6A and 6B) [16,20]. While the porphyrin ring is inserted into a hydrophobic pocket, the
145 ligand binding site remains fairly accessible through an entryway marked by three water
146 molecules that interact with an arginine residue [16]. Oxygen and CO have been shown to bind
147 Fe(II) while CN^- binds Fe(III) on *Rhizobium meliloti* FixL; it has been proposed that the
148 negative shift of the midpoint redox potential observed upon fixation of O_2 , CN^- and imidazole
149 is the consequence of a combination of effects including ligand fixation, heme distortion and
150 ionic interactions of the propionate groups [21]. Structural studies of the oxygen-sensing

151 domain of *B. japonicum* FixL have helped to address important issues relevant to the sensing
152 mechanism [22]. Comparison of the crystal structures of FixL heme domain in its ligand-free
153 and oxygen-bound forms reveals that the binding of dioxygen to the heme iron alters the
154 nonplanarity of the heme, resulting in shifts in the positions of the two heme propionates [22].
155 The movement of the propionate side chains is, in turn, transmitted to the polypeptide via the
156 rearrangements of salt bridges with arginine and histidine residue side chains, affecting the FG
157 loop that is stabilized in an alternative conformation that lies farther from the heme (Figure 6C).
158 These conformational changes then lead to signal transduction [20,22].
159 Contrary that observed in FixL, it has been shown that the heme domain of DosP contains a
160 low-spin heme iron hexacoordinated with a sulfur atom of a methionine residue at the sixth
161 position. This iron coordination is displaced upon O₂ binding, leading to the output signal [17].
162 In the sensor protein DevS from *Mycobacterium tuberculosis*, the ferrous state of the heme Fe
163 in the GAF domain is a typical pentacoordinated Fe(II), while the ferric state is hexacoordinated
164 containing a water molecule ligand at the sixth ligand [19]. Spectro-electrochemical analysis
165 demonstrated that, in contrast to that to FixL, the binding of O₂ to DevS does not change the
166 heme planarity or the propionate interactions with the protein moiety [23].

167

168 2.3 Fe-S cluster -containing PAS domains

169 Fe-S clusters are composed of iron ions and sulfide and are mainly coordinated to the protein
170 moiety via cysteine thiol side chains. These clusters are found in a variety of proteins, including
171 O₂ sensors containing PAS and GAF domains. The sensor kinase NreB from *Staphylococcus*
172 *carneus* binds a [4Fe-4S]²⁺ cluster in a PAS domain liganded by four cysteine residues. Upon
173 reaction with air, the cluster is first degraded to [2Fe-2S]²⁺ and later to Fe hydroxide [24] in a
174 reaction sequence similar to that of the O₂-sensitive transcriptional regulator FNR [25]. As for
175 FNR, it can be hypothesized that the released sulfide ions are oxidized to sulfane and form a
176 persulfide with two of the cysteine ligands of the cluster, allowing sulfur storage and reversion
177 to a [4Fe-4S]²⁺ form cluster in NreB by reduction and repair without involvement of iron-sulfur
178 biosynthesis machinery [26,27]. The sensor kinase AirS of the two-component system AirS-
179 AirR from *Staphylococcus aureus* binds a redox-active [2Fe-2S] cluster critical for kinase
180 activity in a GAF domain liganded by four cysteine residues organized in the consensus motif
181 C-X₇-C-X-C-X₁₇-C. In the [2Fe-2S]²⁺ form oxidized by O₂, AirS is fully active, while the
182 reduced form [2Fe-2S]¹⁺ under anaerobic conditions has minimal kinase activity. Destruction
183 of the cluster by stronger oxidizing agents such as H₂O₂ abolishes kinase activity [28]. Both
184 NreB and AirS bind Fe-S clusters in a PAS or GAF domain for oxygen sensing but their

185 responses to O₂ differ: NreB responds by [4Fe-4S]²⁺/[2Fe-2S]²⁺ conversion while AirS
186 responds by [2Fe-2S]²⁺/[2Fe-2S]¹⁺ oxidation.

187 Recently, a new Fe-S redox regulator OrpR, belonging to the σ⁵⁴-dependent transcriptional
188 regulator family, was characterized from the anaerobic sulfate reducer *Desulfovibrio vulgaris*
189 Hildenborough [29]. OrpR contains a PAS domain that binds a [4Fe-4S]²⁺ cluster under
190 anaerobic conditions. Site-directed mutagenesis demonstrated that three conserved cysteine
191 residues in the PAS domain included in the sequence C-X₈-C-X₃-C were ligands of the Fe-S
192 cluster (Figure 7). The cluster is converted to [3Fe-4S]¹⁺ and Fe³⁺ under mild oxidative
193 conditions, while it is dissembled by O₂. However, both [4Fe-4S]²⁺ and [3Fe-4S]¹⁺ redox states
194 of OrpR are able to bind DNA with no significantly different affinity [29].

195

196 **3. Activity, signal sensing and signal transduction of metal-containing** 197 **PAS/GAF bacterial sensors**

198

199 How do these disparate metal-binding PAS and GAF sensor units regulate the activity of
200 effector domains? This question is addressed in the second part of the review focusing on metal-
201 containing PAS/GAF domains included in TCS and σ⁵⁴-dependent transcriptional regulators.

202

203 3.1. Two-component systems with input metallic PAS/GAF domains

204 TCS systems are the main prokaryote actors sensing environmental changes using histidine
205 kinase (HK) sensing domain (Figure 1A) and a cognate response regulator domain (RR) to
206 mediate the cellular response. The sensing module of HK, which is commonly located in the
207 periplasmic or cytoplasmic spaces, modulates the enzymatic activity of the cytoplasmic effector
208 modules (DHp and CA) via the central HAMP domain (Figure 1A). Except for the PhoQ/PhoP
209 TCS, for which divalent cations such as Mg²⁺ serve as direct signals, other TCSs studied to date
210 exhibit b- and c-type hemes, non-heme iron and iron-sulfur metal cofactors bound to the
211 PAS/GAF domain to sense the signal and to mediate it to the output domain to modulate the
212 activity of the protein. In these disparate sensors, O₂ seems to be the main signal perceived by
213 the metal to activate or inactivate the phosphotransferase activity of HK. The state-of-the-art
214 PAS/GAF metal-containing HK sensors are described below, on the basis of the HK activity in
215 the presence of O₂.

216

217 3.1.1 Repression of TCS metal-containing PAS/GAF bacterial sensors by O₂

218 FixL/FixJ, NreB/NreC and DosS/DosT are cytosolic oxygen-sensing TCSs isolated from
219 *Rhizobium*, Firmicutes species and *Mycobacterium tuberculosis*, respectively [24,30,31].
220 FixL is the sensing domain of FixL/FixJ TCS conserved in α -proteobacteria that consists of
221 two N-terminal tandem PAS domains and a C-terminal HK domain such as in *Bradyrhizobium*
222 *japonicum* [16,32]. In the presence of O₂, O₂ is bound to the b-type heme of the second PAS
223 domain, leading to heme distortion (Figure 6C) that turns off the HK activity [16]. Under
224 hypoxia conditions, O₂ dissociates from the heme, inducing a local conformational change that
225 leads to the autophosphorylation of the HK module and the transfer of phosphate from ATP to
226 the RR FixJ which, in turn, stimulates the expression of target genes (Figure 8) [32].
227 NreB is an O₂ sensor kinase characterized in *Staphylococcus carnosus* and *Staphylococcus*
228 *aureus* that is composed of an N-terminal PAS domain and an HK domain [8,24,33]. Under
229 anoxic conditions, the PAS domain is in the form of [4Fe-4S]²⁺, a state in which NreB has high
230 autokinase activity resulting in RR NreC phosphorylation and target gene transcription (Figure
231 8) [34]. In the presence of O₂, [4Fe-4S]²⁺ is converted into [2Fe-2S]²⁺, leading to a decrease in
232 autokinase activity causing low levels of NreC phosphorylation and gene activation (Figure 8)
233 [24,35]. In parallel and in the absence of nitrate, the GAF-containing domain NreA converts
234 the kinase activity of NreB into phosphatase activity that inactivates NreC; however, no
235 cofactor has been described in association with the GAF domain of NreA [36].
236 DevS and DosT are two cognate O₂ sensor kinases of the DevR transcriptional regulator
237 [37,38]. Two N-terminal GAF domains in tandem are present in both sensors in *M. tuberculosis*.
238 Upon binding of O₂ to the heme-containing GAF module, kinase activity is ceased because of
239 a decrease in kinase activity concomitant with phosphatase-dominant forms of DosT and DevS
240 (Figure 8) [23,39-41]. When the O₂ concentration starts to decrease, DosT first promotes DosR
241 phosphorylation and the transcription of its regulon [23,42]; at lower O₂ concentrations, DosT
242 also activates histidine kinase activity and makes DevR fully phosphorylated. Hence, DosT and
243 DevS work in a two-step adaptation mechanism for hypoxia [23]. NO and CO are also able to
244 activate kinase autophosphorylation [43-45]. In the PAS/GAF metal-containing sensors FixL,
245 NreB, DevS and DosT, the kinase activity is then switched off in the presence of O₂ and is
246 switched on by hypoxia (Figure 8).

247

248 3.1.2 Activation of TCS metal-containing PAS/GAF bacterial sensors by O₂

249 In contrast, three other TCS/PAS metal-containing sensors, AirS/AirR, Aer2 and DosP have
250 been shown to be activated in presence of O₂.

251 AirS/AirR from *Staphylococcus aureus* is a cytosolic oxygen-sensing TCS containing the
252 sensing domain AirS, which is composed of a GAF domain associated with an HK module
253 (Figure 9). Under anaerobic conditions the [2Fe-2S]⁺ cluster form in the GAF domain of AirS
254 switch off kinase activity [28]. Under oxidative conditions (in the presence of O₂, NO or CO),
255 AirS responds to oxidation by converting the [2Fe-2S]⁺ in a [2Fe-2S]²⁺ cluster, a form fully
256 active for phosphorylation and the expression of target genes of the RR AirR (Figure 9) [28].
257 However, prolonged oxidation of AirS leads to the apoform of AirS and results in the loss of
258 kinase activity [8,28].

259 Aer2 is a TCS chemoreceptor combining one (*Pseudomonas aeruginosa*) or two PAS domains
260 (*Vibrio cholerae*) with a poly-HAMP (histidine kinase-adenylyl cyclase-methyl-accepting
261 chemotaxis protein-phosphatase) module [18,46]. The PAS (PAS2 in *V. cholerae*) domain
262 coordinates a b-type heme (Figure 9). In the absence of O₂, the kinase is switched off, whereas
263 the presence of the ligand switches on the kinase, inducing the phosphorylation and activation
264 of chemosensory proteins (Figure 9). The activation is linked to the association of O₂ with the
265 heme group, generating a conformation signal in the PAS domain that is transmitted to the
266 kinase control module [18,46-49].

267 Last, DosP is a b-type heme O₂-sensing phosphodiesterase in *Escherichia coli* that catalyzes
268 the conversion of cyclic-di-GMP to linear di-GMP (Figure 9). Heme b is bound to the N-
269 terminal PAS domain associated with the C-terminal phosphodiesterase catalytic domain. As
270 described above, the association of the ligand (O₂, CO and NO) with heme displaces the iron
271 coordination and induces an increase in the rigidity of the protein structure, leading to signal
272 transduction to the phosphodiesterase domain which is switched on [50-52].

273 Hence, in PAS/GAF metal-containing sensors AirS, Aer2 and DosP, activities of the catalytic
274 domain are switched on in the presence of O₂ (Figure 9).

275

276 3.1.3 Repression of TCS-containing PAS/GAF bacterial sensors by direct metal-sensing.

277 The TCSs described above exhibit b- and c-type hemes, non-heme iron and iron-sulfur metal
278 cofactors bound to the PAS/GAF domain to sense the O₂ signal PAS/GAF domain. TCS,
279 PhoQ/PhoP and Walk/WalR are two PAS containing TCSs in which metal serves as a direct
280 signal.

281 PhoQ is a transmembrane sensor kinase, found in enterobacteria, composed of a periplasmic
282 PAS domain and a C-terminal catalytic HK domain located in the cytoplasm (Figure 10). Under
283 physiological conditions, Mg²⁺ is bound to the PAS domain, dephosphorylates its cognate RR
284 PhoP resulting in the inactivation of PhoQ [53]. In Mg²⁺-limited conditions, the metal

285 dissociates from the PAS domain, and a reorientation of PhoQ relative to the membrane is
286 observed. This change corresponds to the activation of PhoP in the cytoplasm through a classic
287 phosphotransfer pathway in these TCSs (Figure 10) [53,54]. Other divalent metal ligands such
288 as Ni^{2+} , Mn^{2+} and Ca^{2+} , when associated to PhoQ, can also inactivate the kinase [55].

289 WalKR regulates peptidoglycan synthesis and is essential in *Staphylococcus aureus* [56].
290 WalK, the HK sensor, comprises two N-terminal tandem PAS domains and a C-terminal HK
291 domain. One PAS is located in the extracellular space, and another is located in the cytoplasm
292 (Figure 10) [57]. Cytoplasmic PAS has recently been shown to bind Zn^{2+} , which directly
293 influences the activation status of the protein [15]. In the absence of Zn^{2+} the
294 autophosphorylation of WalK is favored, which leads to phosphotransfer to the RR WalR and
295 binding of the RR on its target sequences. In the presence of Zn^{2+} , cation binding influences the
296 positioning between the PAS and HK domains (Figure 5C), a conformation that decreases the
297 autophosphorylation of WalK [15].

298

299 3.2 σ^{54} -Dependent activators with input metallic GAF/PAS domains

300 σ^{54} -dependent activators control σ^{54} -dependent transcription in response to environmental
301 signals. These activator proteins generally consist of three domains: an N-terminal regulatory
302 domain that senses the signal, a central AAA⁺ domain responsible for ATP hydrolysis and a C-
303 terminal DNA-binding domain (Figure 1B). Three σ^{54} -dependent activators contain a
304 PAS/GAF sensory domain, NorR, AdhR and OrpR.

305 Binding of NO to the non-heme iron of the NorR activator from *E. coli* stimulates the ATPase
306 activity of the central domain of NorR, enabling the activation of transcription by σ^{54} -RNA
307 polymerase (Figure 11) [10]. Prior to NO activation, the GAF domain is located above the
308 AAA⁺ domain preventing ATP hydrolysis [58]. Upon activation, a mononitrosyl iron complex
309 is formed, and the GAF domain relocates downwards to the periphery of the AAA⁺ domain,
310 making the AAA⁺ domain accessible for ATP hydrolysis and σ^{54} RNA polymerase (Figure 11)
311 [10,58].

312 The AdhR activator from *Clostridium beijerinckii* also possesses a non-heme iron center within
313 its N-terminal GAF domain (Figure 11). Under oxidative stress, the tandem GAF and PAS
314 domains repress the accessibility of the AAA⁺ domain in AdhR [59]. Binding of Fe^{2+} in
315 anaerobic conditions relieves the repression of AAA⁺ and stimulates ATPase activity allowing
316 AdhR to stimulate transcription (Figure 11) [59].

317 Lastly characterized, the OrpR activator in *Desulfovibrio vulgaris* Hildenborough contains a
318 $[\text{4Fe-4S}]^{2+}$ cluster in its N-terminal PAS domain (Figure 11). In anaerobiosis OrpR is activated

319 and stimulates the OrpR regulon [29,60,61]. Increasing the redox potential turns off the OrpR
320 activity via the redox-sensitive $[4\text{Fe-4S}]^{2+}$ in the PAS domain (Figure 11) [29]. The PAS
321 domain negatively regulates the activity of OrpR under oxidative conditions, but its role on the
322 AAA⁺ domain remains to be discovered [29].

323

324 **4. Conclusion**

325 Despite their invariant structure, the PAS/GAF domains bind disparate metal cofactors with
326 precise coordination and high specificity concomitant with their extensive sequence diversity.
327 O₂ and redox potential seem to be the favorite signaling stimuli of these sensors, but gases such
328 as NO or CO can also mediate their induction. Stimuli induce subtle conformational changes
329 concentrated in cofactor-binding sites, allowing signal transduction to the effector output
330 modules and leading to cellular response.

331 PAS/GAF sensors can regulate the activities of very different effector domains through either
332 their redox state or their structural change upon ligand binding, which induces conformational
333 changes. The metal-containing PAS/GAF domains characterized to date are coupled to histidine
334 kinases of two-component signaling systems and σ^{54} -dependent transcription factors. In both
335 cases, signal-induced conformational changes are necessary to transduce the signal to the
336 effector domains. Even if these conformational changes are protein-dependent, the mechanism
337 adopted to regulate the activity of the output domain seems to be completely correlated with
338 the class of effector domain. In HK, the different structural conformations of the cofactor pocket
339 linked to the absence or presence of a ligand modulate the phosphorylation state of HK and its
340 activity. In σ^{54} -dependent activators, signal-induced structural conformation changes in
341 PAS/GAF domains have been shown to impact the accessibility of the AAA⁺ domain for ATP
342 hydrolysis and σ^{54} RNA polymerase.

343 Metal-containing PAS/GAS domains, as other PAS/GAF domains, offer great possibilities for
344 coupling a broad range of ligand binding to various cellular responses, and it is very likely that
345 they have not yet revealed all their secrets. For example, 141 PAS domains have been identified
346 in the genome of the deltaproteobacterium *Desulfovibrio* but only two have been characterized
347 to date. Moreover, the first heme-binding PAS domain accommodating enzymatic activity has
348 been reported, which suggests that other PAS enzymes are likely to exist [62].

349 More generally, in addition to be signal sensing proteins, the bacterial PAS/GAF with and
350 without cofactors have been shown to be involved in signal modulation, transduction,
351 dimerization, protein interaction and cellular localization [63]. Advantageously to other
352 signaling proteins, PAS/GAF-containing proteins are associated to a wide variety of domains

353 such as HKs, σ^{54} -dependent activators, diguanylate cyclases/phosphodiesterases and methyl-
354 accepting chemotaxis proteins (this list is not exhaustive). Extracellular and intracellular
355 localization, the incredible versatility of signal sensed (light, gases, redox potential, metals,
356 fatty acids, carbohydrates...) make PAS/GAF domains versatile and unique systems for rapid
357 adaptation to environmental changes and ensure survival of microorganisms.

358

359

360 **Figure legends:**

361 **Figure 1: Schematic representation of the protein architecture and signal transduction of**
362 **canonical PAS/GAF-containing sensor histidine kinases and σ^{54} -dependent**
363 **transcriptional regulators.** (A) Histidine Kinases SHKs are mostly dimeric and they are
364 basically organized in three structural elements: the sensing PAS/GAF core (red) able to bind
365 a metal (yellow) followed by the four-alpha-helical HAMP region connected to the helical
366 effector module which comprises the DHp domain (Dimerization and phospho-accepting
367 Histidine) (pink) and the catalytic domain (CA) (light blue). (B) Canonical σ^{54} -dependent
368 transcriptional regulators are mostly hexameric and contain three domains: the N-terminal
369 sensing domain (red), the central AAA+ module responsible for ATPase activity (blue) and the
370 C-terminal HTH (Helix Turn Helix) DNA binding domain (green).

371

372 **Figure 2: Structural comparison PAS/GAF domain.** (A) Proposed three-dimensional PAS
373 domain based on the PYP (Phosphoactive Yellow Protein) structure, obtained from Taylor and
374 colleagues (PDB id: 3PYP) [11]. The PAS domain is organized in four main structural
375 elements: the PAS core (red), the β -scaffold (green), the helical connector (blue) and the N-
376 terminal cap (yellow). (B) Structure of the GAF domain based on the YGK9 protein (PDB id:
377 3kO6). Regions that can be superimposed between PYP and YGK9 structure within 3 Å are
378 colored in red.

379

380 **Figure 3: Proposed structural model of Fe center in the NorR GAF domain.** (A) Overview
381 of the model showing the position of the iron in the GAF domain. (B) View of the ferrous iron
382 center showing the proposed iron ligands. The Arg75 residue is the most likely to undergo
383 ligand displacement upon NO binding. Figure was obtained from Tucker and colleagues [11].

384

385 **Figure 4: Dimeric structure of the PhoQ sensor domain from *S. typhimurium*.** Red-colored
386 side-chains are negatively charged residues and gray balls represent Ca^{2+} cations (PDB id:
387 1yax) [12].

388

389 **Figure 5: Structure of the PAS domain of the WalK sensor from *Staphylococcus aureus*.**
390 (A) Entire PAS domain; the bound Zn^{2+} is shown as a gray sphere and its coordinating residues
391 are shown as cyan sticks. (B) Focus on the Zn^{2+} -binding site; the atoms that contribute to the
392 interaction with Zn^{2+} are in spheres (PDB id: 4mn5) [15]. (C) Molecular modelling of WalK in
393 the presence (1) or absence (2) of Zn^{2+} showing the predicted conformational changes induced

394 in the WalK PAS and catalytic (CAT) domains upon metal binding; obtained from Monk and
395 colleagues [15].

396

397 **Figure 6: Structures of ligand-free FixL heme domains.** (A) from *Rhizobium meliloti* (PDB
398 id: 1d06) [20](B) from *Bradyrhizobium japonicum* (PDB id: 1drm) [16]. (C) Superposition of
399 the crystal structures of the *Bradyrhizobium japonicum* oxygen-bound (bronze) (PDB id: 1dp6)
400 and ligand-free (blue) (PDB id: 1drm) FixL heme domain [22]. Dioxygen is in red.

401

402 **Figure 7: Structural model of the PAS domain from OrpR.** The cysteine residues involved
403 in cluster binding are indicated; obtained from Fievet and colleagues [29].

404

405 **Figure 8: Organization and O₂ repression of TCS metal-containing PAS/GAF sensors.**
406 Domains organization and model of inactivation by O₂ of the metal-containing PAS/GAF TCS
407 sensors FixL in *Bradyrhizobium japonicum*, NreB in *Staphylococcus carnosus* and DosS/DosT
408 in *Mycobacterium tuberculosis*.

409

410 **Figure 9: Organization and O₂ activation of TCS metal-containing PAS/GAF sensors.**
411 Domains organization and model of activation by O₂ of the metal-containing PAS/GAF TCS
412 sensors AirS in *Staphylococcus aureus*, Aer2 in *Pseudomonas aeruginosa* and DosP in
413 *Escherichia coli*.

414

415 **Figure 10: Repression of TCS-containing PAS/GAF sensors by direct metal-sensing.**
416 Domains organization and model of inactivation by cations of the metal-containing PAS/GAF
417 TCS sensors PhoQ in enterobacteria and WalK in *Staphylococcus aureus*.

418

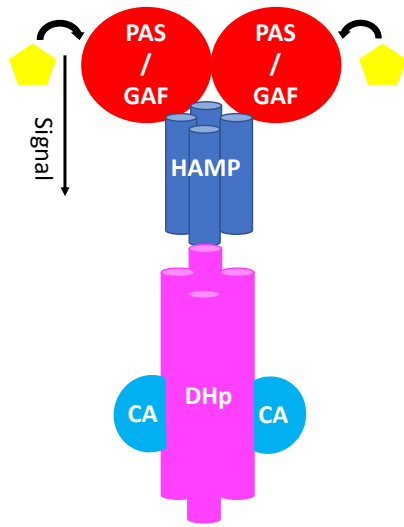
419 **Figure 11: σ^{54} -Dependent activators with input metallic GAF/PAS domains.** Domains
420 organization and model of activation/inactivation of the metal-containing PAS/GAF σ^{54} -
421 dependent activators NorR in *E. coli*, AdhR in *Clostridium beijerinckii* and OrpR in
422 *Desulfovibrio vulgaris* Hildenborough.

423

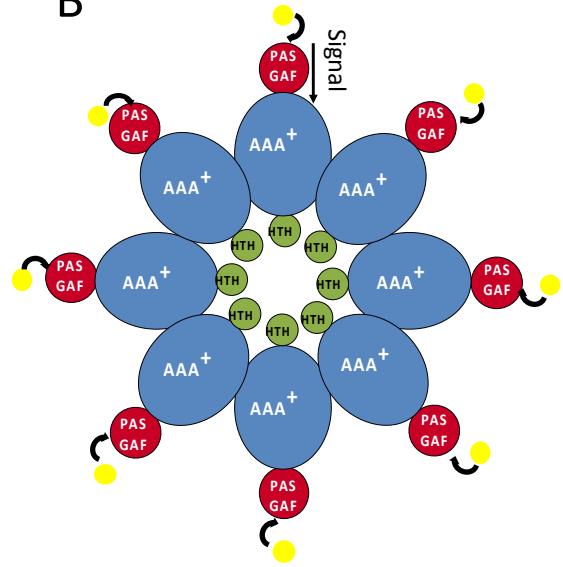
424

425 **Figure 1 :**
426

A



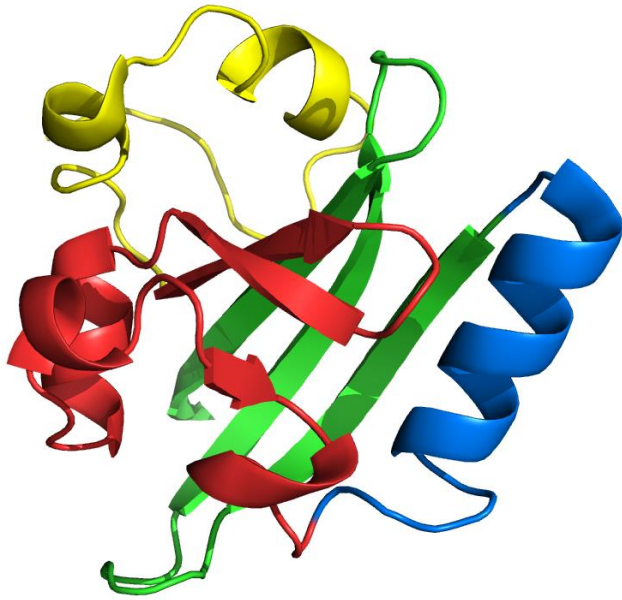
B



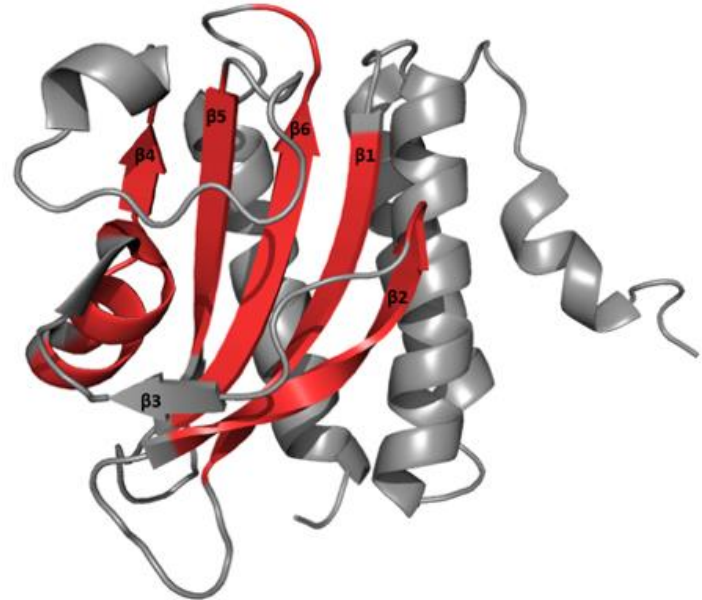
427
428

429 **Figure 2:**
430
431

A



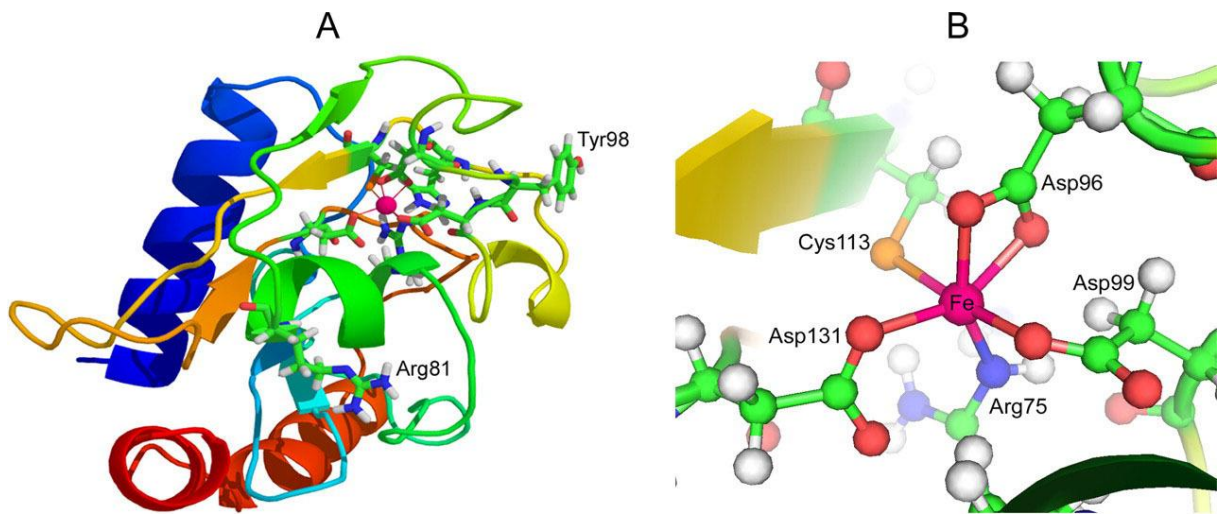
B



435
436
437
438
439
440
441
442
443
444
445
446
447
448
449
450
451
452
453
454
455
456
457

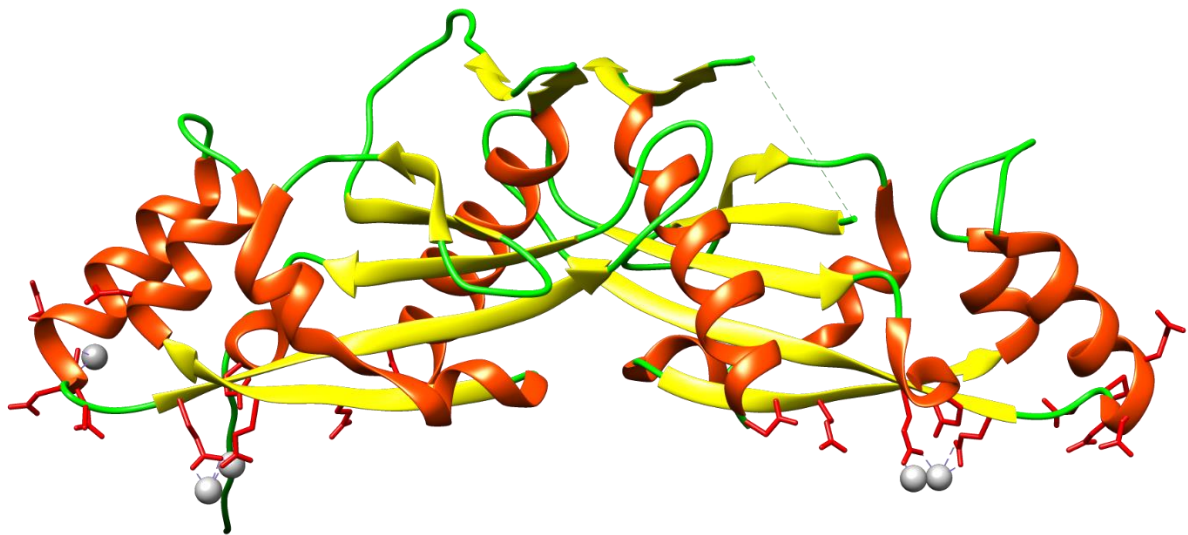
458 **Figure 3 :**

459
460
461
462
463
464
465
466
467
468
469
470



471 **Figure 4**

472
473
474
475
476
477
478
479
480
481
482
483
484
485
486
487
488
489
490
491
492
493
494
495
496
497
498
499
500
501
502
503



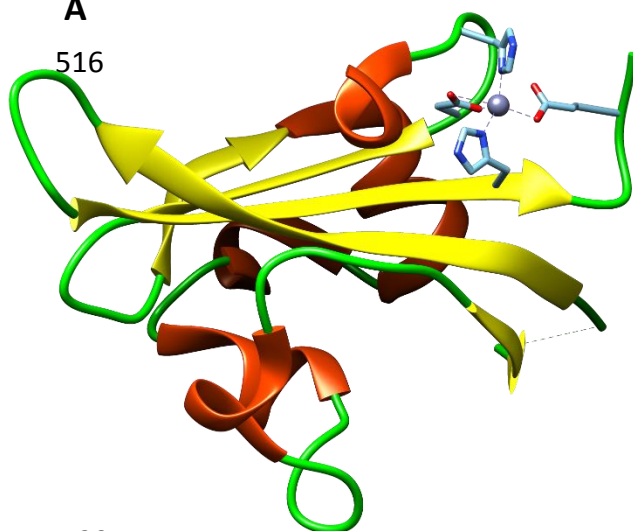
504
505
506
507
508
509
510
511
512

Figure 5

513

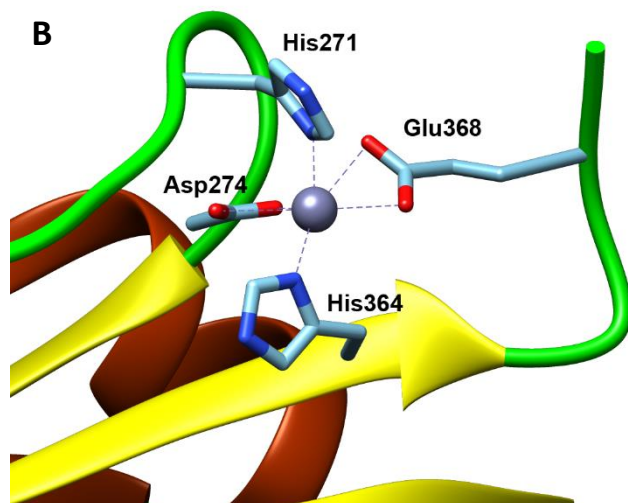
A

516



517
518
519
520
521
522
523
524
525
526
527
528

B

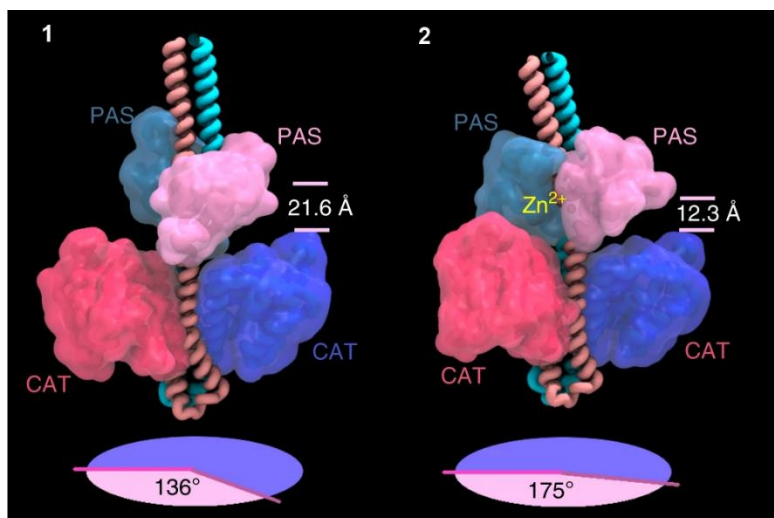


529

C

531

532
533
534
535
536
537
538
539
540
541
542
543
544
545
546
547
548
549
550
551
552



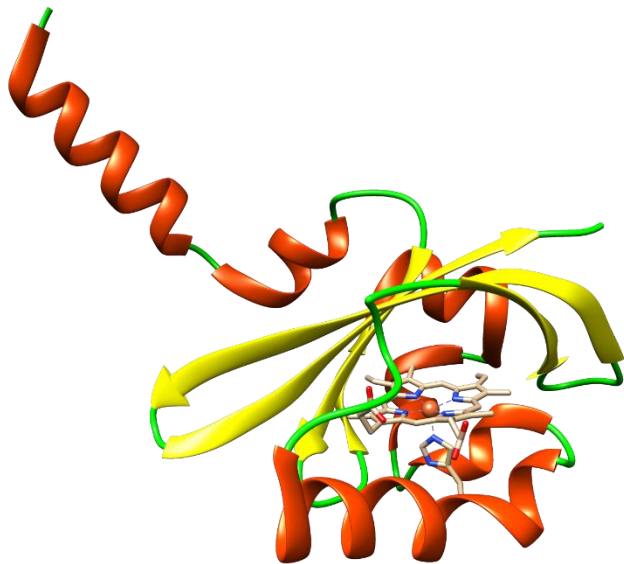
553 **Figure 6 :**

554
555

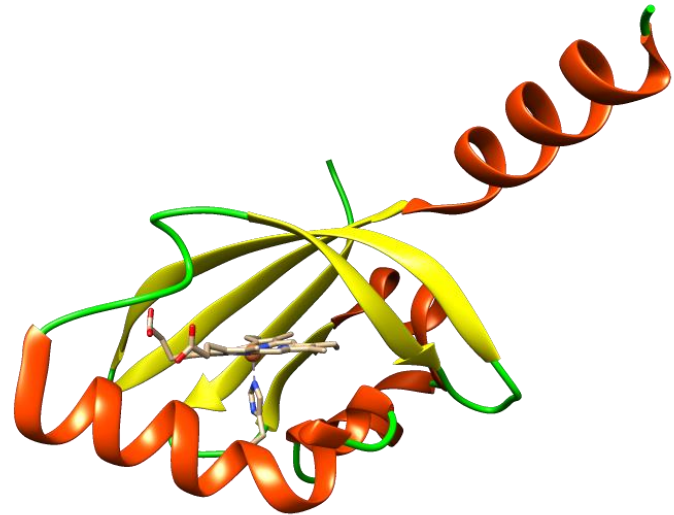
556

A

559
560
561
562
563
564
565
566
567
568
569
570
571
572
573
574
575
576

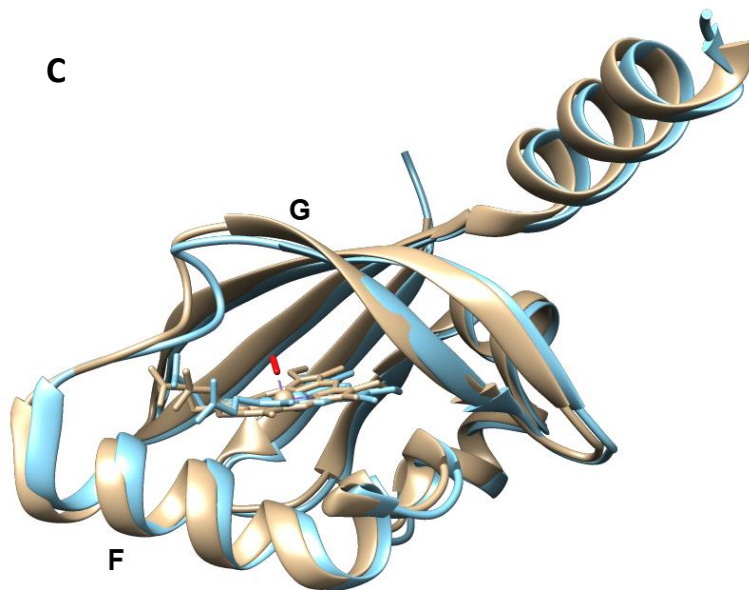


B



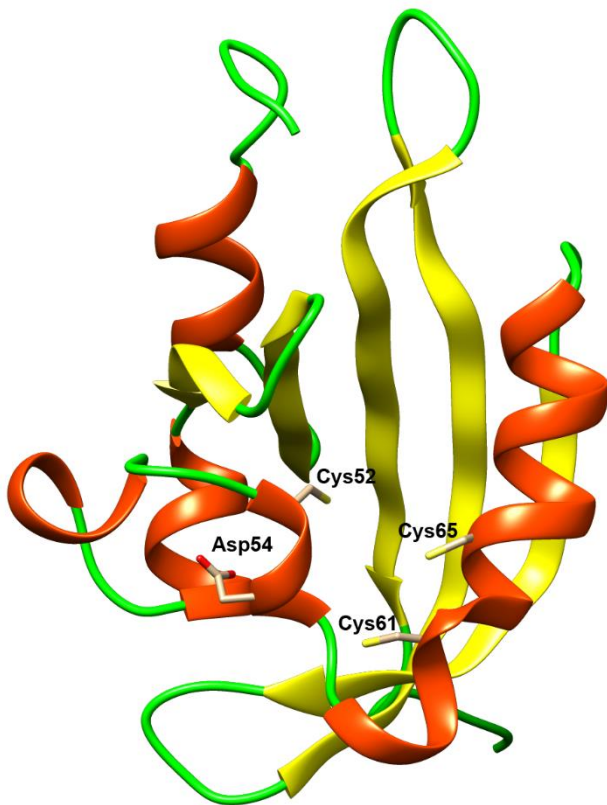
C

580
581
582
583
584
585
586
587
588
589
590
591
592
593
594
595
596
597
598
599
600

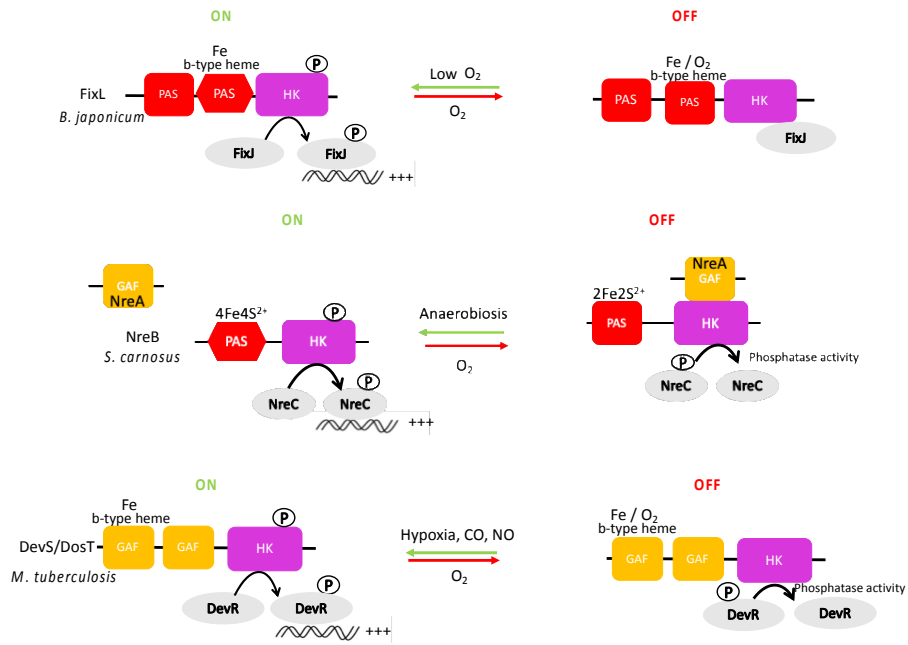


601 **Figure 7**

602
603
604
605
606
607
608
609
610
611
612
613
614
615
616
617
618
619
620
621
622
623
624
625
626
627
628
629

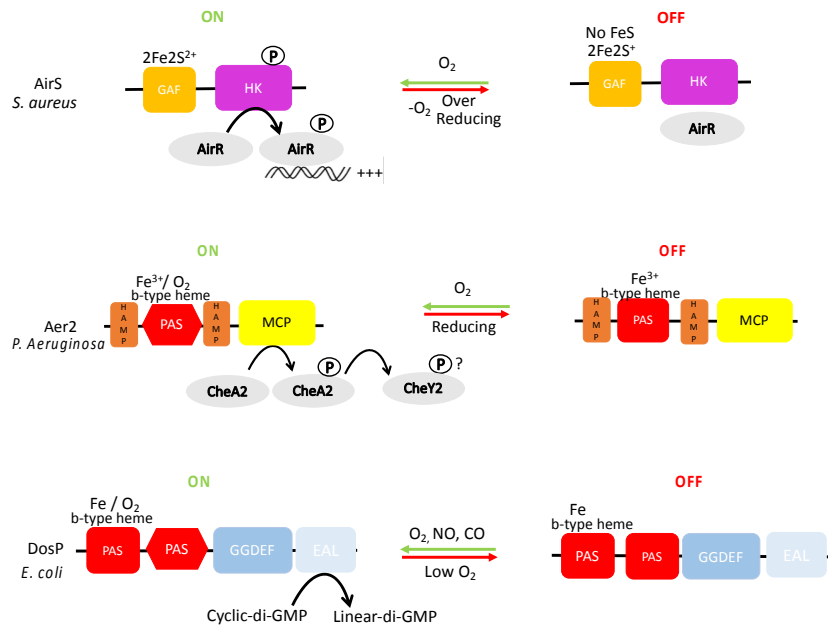


630 Figure 8:
631
632



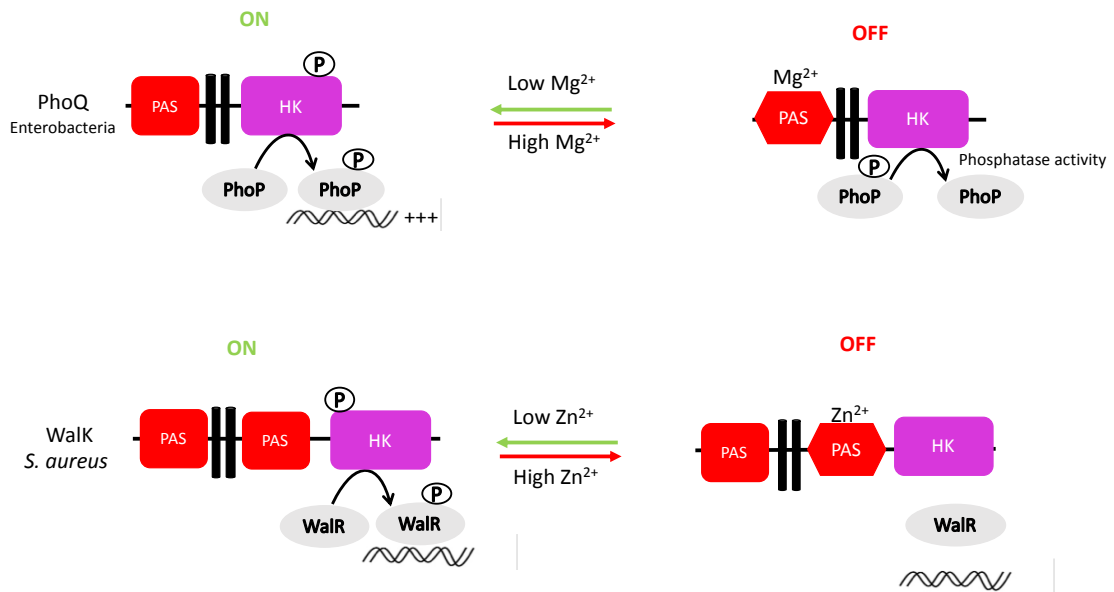
633
634

635 Figure 9:
636



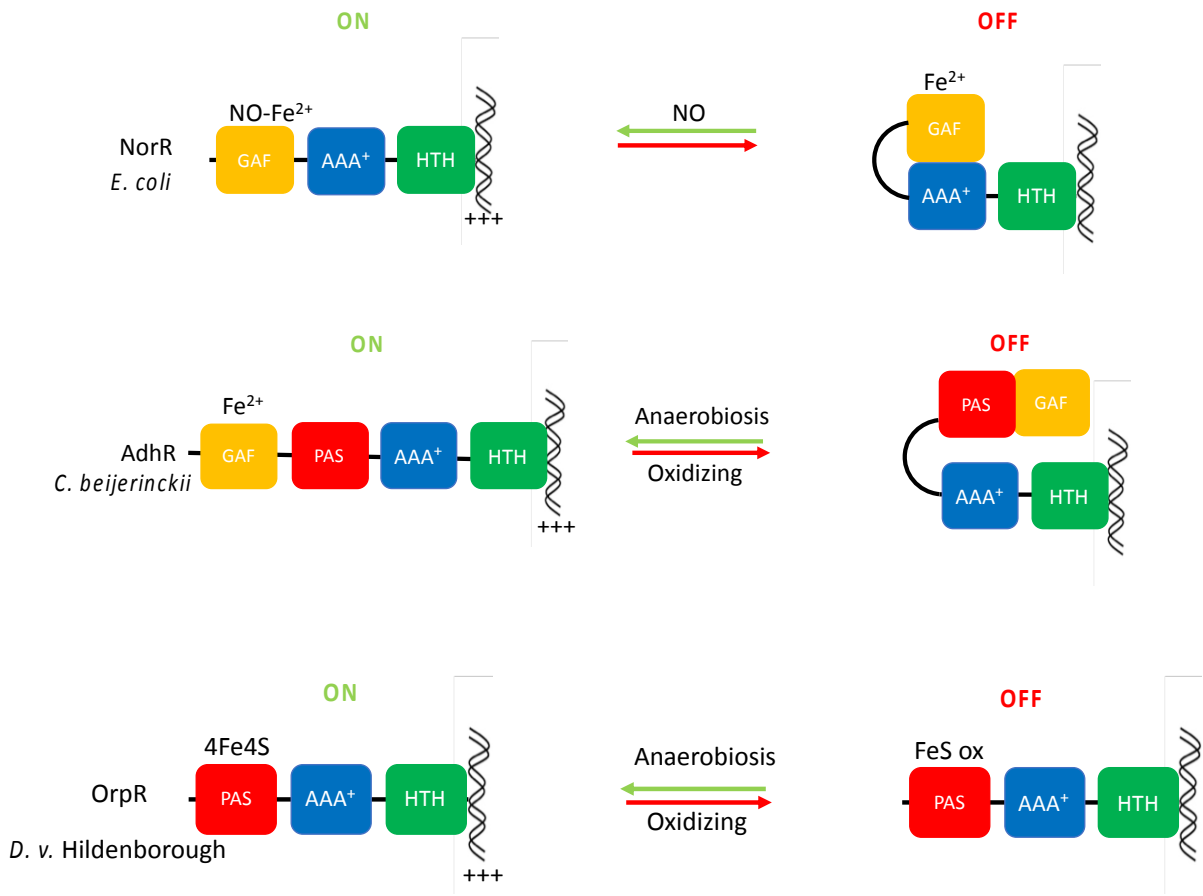
637
638
639
640
641
642

643 Figure 10:
644
645



646
647
648
649
650

651 Figure 11:
652



653
654

655 **References:**

656

- 657 [1] L. Aravind, C. Ponting, The GAF domain: an evolutionary link between diverse
658 phototransducing proteins, *Trends in biochemical sciences* 22 (1997). 10.1016/s0968-
659 0004(97)01148-1.
- 660 [2] J. Henry, S. Crosson, Ligand-binding PAS domains in a genomic, cellular, and structural
661 context, *Annual review of microbiology* 65 (2011). 10.1146/annurev-micro-121809-151631.
- 662 [3] A. Möglich, R. Ayers, K. Moffat, Structure and signaling mechanism of Per-ARNT-Sim
663 domains, *Structure (London, England : 1993)* 17 (2009). 10.1016/j.str.2009.08.011.
- 664 [4] B. Taylor, I. Zhulin, PAS domains: internal sensors of oxygen, redox potential, and light,
665 *Microbiology and molecular biology reviews : MMBR* 63 (1999).
- 666 [5] R. Finn, J. Mistry, B. Schuster-Böckler, S. Griffiths-Jones, V. Hollich, T. Lassmann, S. Moxon,
667 M. Marshall, A. Khanna, R. Durbin, S. Eddy, E. Sonnhammer, A. Bateman, Pfam: clans, web
668 tools and services, *Nucleic acids research* 34 (2006). 10.1093/nar/gkj149.
- 669 [6] Y. Ho, L. Burden, J. Hurley, Structure of the GAF domain, a ubiquitous signaling motif and
670 a new class of cyclic GMP receptor, *The EMBO journal* 19 (2000). 10.1093/emboj/19.20.5288.
- 671 [7] G. Sharma, R. Parales, M. Singer, In silico characterization of a novel putative aerotaxis
672 chemosensory system in the myxobacterium, *Coralloccoccus coralloides*, *BMC genomics* 19
673 (2018). 10.1186/s12864-018-5151-6.
- 674 [8] G. Unden, S. Nilkens, M. Singenstreu, Bacterial sensor kinases using Fe-S cluster binding
675 PAS or GAF domains for O₂ sensing, *Dalton transactions (Cambridge, England : 2003)* 42
676 (2013). 10.1039/c2dt32089d.
- 677 [9] M. Bush, T. Ghosh, N. Tucker, X. Zhang, R. Dixon, Transcriptional regulation by the
678 dedicated nitric oxide sensor, NorR: a route towards NO detoxification, *Biochemical Society*
679 *transactions* 39 (2011). 10.1042/BST0390289.
- 680 [10] B. D'Autréaux, N. Tucker, R. Dixon, S. Spiro, A non-haem iron centre in the transcription
681 factor NorR senses nitric oxide, *Nature* 437 (2005). 10.1038/nature03953.
- 682 [11] N. Tucker, B. D'Autréaux, F. Yousafzai, S. Fairhurst, S. Spiro, R. Dixon, Analysis of the nitric
683 oxide-sensing non-heme iron center in the NorR regulatory protein, *The Journal of biological*
684 *chemistry* 283 (2008). 10.1074/jbc.M705850200.
- 685 [12] U. Cho, M. Bader, M. Amaya, M. Daley, R. Klevit, S. Miller, W. Xu, Metal bridges between
686 the PhoQ sensor domain and the membrane regulate transmembrane signaling, *Journal of*
687 *molecular biology* 356 (2006). 10.1016/j.jmb.2005.12.032.
- 688 [13] J. Cheung, C. Bingman, M. Reyngold, W. Hendrickson, C. Waldburger, Crystal structure of
689 a functional dimer of the PhoQ sensor domain, *The Journal of biological chemistry* 283 (2008).
690 10.1074/jbc.M710592200.
- 691 [14] S. Biswas, A. Adhikari, A. Mukherjee, S. Das, S. Adak, Regulation of Leishmania major PAS
692 domain-containing phosphoglycerate kinase by cofactor Mg²⁺ ion at neutral pH, *The FEBS*
693 *journal* 287 (2020). 10.1111/febs.15305.
- 694 [15] I. Monk, N. Shaikh, S. Begg, M. Gajdiss, L. Sharkey, J. Lee, S. Pidot, T. Seemann, M. Kuiper,
695 B. Winnen, R. Hvorup, B. Collins, G. Bierbaum, S. Udagedara, J. Morey, N. Pulyani, B. Howden,
696 M. Maher, C. McDevitt, G. King, T. Stinear, Zinc-binding to the cytoplasmic PAS domain
697 regulates the essential Walk histidine kinase of *Staphylococcus aureus*, *Nature*
698 *communications* 10 (2019). 10.1038/s41467-019-10932-4.
- 699 [16] W. Gong, H. B, S. Mansy, G. Gonzalez, M. Gilles-Gonzalez, M. Chan, Structure of a
700 biological oxygen sensor: a new mechanism for heme-driven signal transduction, *Proceedings*

701 of the National Academy of Sciences of the United States of America 95 (1998).
702 10.1073/pnas.95.26.15177.

703 [17] H. Park, C. Suquet, J. Satterlee, C. Kang, Insights into signal transduction involving PAS
704 domain oxygen-sensing heme proteins from the X-ray crystal structure of *Escherichia coli* Dos
705 heme domain (Ec DosH), *Biochemistry* 43 (2004). 10.1021/bi035980p.

706 [18] S. Greer-Phillips, N. Sukomon, T. Chua, M. Johnson, B. Crane, K. Watts, THE AER2
707 RECEPTOR FROM *VIBRIO CHOLERAE* IS A DUAL PAS-HEME OXYGEN SENSOR, *Molecular*
708 *microbiology* (2018). 10.1111/mmi.13978.

709 [19] S. Sardival, S. Kendall, F. Movahedzadeh, S. Rison, N. Stoker, S. Djordjevic, A GAF domain
710 in the hypoxia/NO-inducible *Mycobacterium tuberculosis* DosS protein binds haem, *Journal of*
711 *molecular biology* 353 (2005). 10.1016/j.jmb.2005.09.011.

712 [20] H. Miyatake, M. Mukai, S. Park, S. Adachi, K. Tamura, H. Nakamura, K. Nakamura, T.
713 Tsuchiya, T. Iizuka, Y. Shiro, Sensory mechanism of oxygen sensor FixL from *Rhizobium*
714 *meliloti*: crystallographic, mutagenesis and resonance Raman spectroscopic studies, *Journal*
715 *of molecular biology* 301 (2000). 10.1006/jmbi.2000.3954.

716 [21] N. Honorio-Felício, M. Carepo, T. de F Paulo, L. de França Lopes, E. Sousa, I. Diógenes, P.
717 Bernhardt, The Heme-Based Oxygen Sensor *Rhizobium etli* FixL: Influence of Auxiliary Ligands
718 on Heme Redox Potential and Implications on the Enzyme Activity, *Journal of inorganic*
719 *biochemistry* 164 (2016). 10.1016/j.jinorgbio.2016.08.009.

720 [22] W. Gong, B. Hao, M. Chan, New mechanistic insights from structural studies of the
721 oxygen-sensing domain of *Bradyrhizobium japonicum* FixL, *Biochemistry* 39 (2000).
722 10.1021/bi992346w.

723 [23] G. Barreto, M. Carepo, A. Gondim, W. Guimarães, L. Lopes, P. Bernhardt, T. Paulo, E.
724 Sousa, I. Diógenes, A spectroelectrochemical investigation of the heme-based sensor DevS
725 from *Mycobacterium tuberculosis*: a redox versus oxygen sensor, *The FEBS journal* 286 (2019).
726 10.1111/febs.14974.

727 [24] M. Müllner, O. Hammel, B. Mienert, S. Schlag, E. Bill, G. Udden, A PAS domain with an
728 oxygen labile [4Fe-4S](2+) cluster in the oxygen sensor kinase NreB of *Staphylococcus*
729 *carneus*, *Biochemistry* 47 (2008). 10.1021/bi8014086.

730 [25] P. Kiley, H. Beinert, Oxygen sensing by the global regulator, FNR: the role of the iron-sulfur
731 cluster, *FEMS microbiology reviews* 22 (1998). 10.1111/j.1574-6976.1998.tb00375.x.

732 [26] C. Barth, M. Weiss, M. Roettger, W. Martin, G. Udden, Origin and phylogenetic
733 relationships of [4Fe-4S]-containing O₂ sensors of bacteria, *Environmental microbiology* 20
734 (2018). 10.1111/1462-2920.14411.

735 [27] B. Zhang, J. Crack, S. Subramanian, J. Green, A. Thomson, N. Le Brun, M. Johnson,
736 Reversible cycling between cysteine persulfide-ligated [2Fe-2S] and cysteine-ligated [4Fe-4S]
737 clusters in the FNR regulatory protein, *Proceedings of the National Academy of Sciences of*
738 *the United States of America* 109 (2012). 10.1073/pnas.1208787109.

739 [28] F. Sun, J. Q. M. Jones, X. Deng, H. Liang, B. Frank, J. Telser, S. Peterson, T. Bae, C. He, AirSR,
740 a [2Fe-2S] cluster-containing two-component system, mediates global oxygen sensing and
741 redox signaling in *Staphylococcus aureus*, *Journal of the American Chemical Society* 134
742 (2012). 10.1021/ja2071835.

743 [29] A. Fiévet, M. Merrouch, G. Brasseur, D. Eve, E. Biondi, O. Valette, S. Pauleta, A. Dolla, Z.
744 Dermoun, B. Burlat, C. Aubert, OrpR is a σ^{54} -dependent activator using an iron-sulfur cluster
745 for redox sensing in *Desulfovibrio vulgaris* Hildenborough, *Molecular microbiology* (2021).
746 10.1111/mmi.14705.

747 [30] M. Gilles-Gonzalez, G. Gonzalez, Regulation of the kinase activity of heme protein FixL
748 from the two-component system FixL/FixJ of *Rhizobium meliloti*, *The Journal of biological*
749 *chemistry* 268 (1993).

750 [31] E. Monson, M. Weinstein, G. Ditta, D. Helinski, The FixL protein of *Rhizobium meliloti* can
751 be separated into a heme-binding oxygen-sensing domain and a functional C-terminal kinase
752 domain, *Proceedings of the National Academy of Sciences of the United States of America* 89
753 (1992). 10.1073/pnas.89.10.4280.

754 [32] G. Wright, A. Saeki, T. Hikima, Y. Nishizono, T. Hisano, M. Kamaya, K. Nukina, H. Nishitani,
755 H. Nakamura, M. Yamamoto, S. Antonyuk, S. Hasnain, Y. Shiro, H. Sawai, Architecture of the
756 complete oxygen-sensing FixL-FixJ two-component signal transduction system, *Science*
757 *signaling* 11 (2018). 10.1126/scisignal.aaq0825.

758 [33] F. Reinhart, A. Huber, R. Thiele, G. Uden, Response of the oxygen sensor NreB to air in
759 vivo: Fe-S-containing NreB and apo-NreB in aerobically and anaerobically growing
760 *Staphylococcus carnosus*, *Journal of bacteriology* 192 (2010). 10.1128/JB.01248-09.

761 [34] G. Uden, R. Klein, Sensing of O₂ and nitrate by bacteria: alternative strategies for
762 transcriptional regulation of nitrate respiration by O₂ and nitrate, *Environmental*
763 *microbiology* 23 (2021). 10.1111/1462-2920.15293.

764 [35] S. Nilkens, M. Koch-Singenstreu, V. Niemann, F. Götz, T. Stehle, G. Uden, Nitrate/oxygen
765 co-sensing by an NreA/NreB sensor complex of *Staphylococcus carnosus*, *Molecular*
766 *microbiology* 91 (2014). 10.1111/mmi.12464.

767 [36] R. Klein, A. Kretzschmar, G. Uden, Control of the bifunctional O₂-sensor kinase NreB of
768 *Staphylococcus carnosus* by the nitrate sensor NreA: Switching from kinase to phosphatase
769 state, *Molecular microbiology* 113 (2020). 10.1111/mmi.14425.

770 [37] D. Roberts, R. Liao, G. Wisedchaisri, W. Hol, D. Sherman, Two sensor kinases contribute
771 to the hypoxic response of *Mycobacterium tuberculosis*, *The Journal of biological chemistry*
772 279 (2004). 10.1074/jbc.M401230200.

773 [38] D. Saini, V. Malhotra, D. Dey, N. Pant, T. Das, J. Tyagi, DevR-DevS is a bona fide two-
774 component system of *Mycobacterium tuberculosis* that is hypoxia-responsive in the absence
775 of the DNA-binding domain of DevR, *Microbiology (Reading, England)* 150 (2004).
776 10.1099/mic.0.26218-0.

777 [39] K. Kaur, P. Kumari, S. Sharma, S. Sehgal, J. Tyagi, DevS/DosS sensor is bifunctional and its
778 phosphatase activity precludes aerobic DevR/DosR regulon expression in *Mycobacterium*
779 *tuberculosis*, *The FEBS journal* 283 (2016). 10.1111/febs.13787.

780 [40] E. Sousa, G. Gonzalez, M. Gilles-Gonzalez, Target DNA stabilizes *Mycobacterium*
781 *tuberculosis* DevR/DosR phosphorylation by the full-length oxygen sensors DevS/DosS and
782 DosT, *The FEBS journal* 284 (2017). 10.1111/febs.14284.

783 [41] P. Kumari, S. Kumar, K. Kaur, U. Gupta, S. Bhagyawant, J. Tyagi, Phosphatase-defective
784 DevS sensor kinase mutants permit constitutive expression of DevR-regulated dormancy
785 genes in *Mycobacterium tuberculosis*, *The Biochemical journal* 477 (2020).
786 10.1042/BCJ20200113.

787 [42] A. Vashist, R.D. Prithvi, U. Gupta, R. Bhat, J. Tyagi, The α 10 helix of DevR, the
788 *Mycobacterium tuberculosis* dormancy response regulator, regulates its DNA binding and
789 activity, *The FEBS journal* 283 (2016). 10.1111/febs.13664.

790 [43] H. Park, K. Guinn, M. Harrell, R. Liao, M. Voskuil, M. Tompa, G. Schoolnik, D. Sherman,
791 Rv3133c/dosR is a transcription factor that mediates the hypoxic response of *Mycobacterium*
792 *tuberculosis*, *Molecular microbiology* 48 (2003). 10.1046/j.1365-2958.2003.03474.x.

793 [44] M. Voskuil, D. Schnappinger, K. Visconti, M. Harrell, G. Dolganov, D. Sherman, G.
794 Schoolnik, Inhibition of respiration by nitric oxide induces a Mycobacterium tuberculosis
795 dormancy program, *The Journal of experimental medicine* 198 (2003).
796 10.1084/jem.20030205.

797 [45] M. Shiloh, P. Manzanillo, J. Cox, Mycobacterium tuberculosis senses host-derived carbon
798 monoxide during macrophage infection, *Cell host & microbe* 3 (2008).
799 10.1016/j.chom.2008.03.007.

800 [46] K. Watts, M. Johnson, B. Taylor, Different conformations of the kinase-on and kinase-off
801 signaling states in the Aer HAMP domain, *Journal of bacteriology* 193 (2011).
802 10.1128/JB.01069-10.

803 [47] M. Airola, D. Huh, N. Sukomon, J. Widom, R. Sircar, P. Borbat, J. Freed, K. Watts, B. Crane,
804 Architecture of the soluble receptor Aer2 indicates an in-line mechanism for PAS and HAMP
805 domain signaling, *Journal of molecular biology* 425 (2013). 10.1016/j.jmb.2012.12.011.

806 [48] H. Sawai, H. Sugimoto, Y. Shiro, H. Ishikawa, Y. Mizutani, S. Aono, Structural basis for
807 oxygen sensing and signal transduction of the heme-based sensor protein Aer2 from
808 *Pseudomonas aeruginosa*, *Chemical communications (Cambridge, England)* 48 (2012).
809 10.1039/c2cc32549g.

810 [49] D. Garcia, E. Orillard, M. Johnson, K. Watts, Gas Sensing and Signaling in the PAS-Heme
811 Domain of the *Pseudomonas aeruginosa* Aer2 Receptor, *Journal of bacteriology* 199 (2017).
812 10.1128/JB.00003-17.

813 [50] T. Shimizu, The Heme-Based Oxygen-Sensor Phosphodiesterase Ec DOS (DosP): Structure-
814 Function Relationships, *Biosensors* 3 (2013). 10.3390/bios3020211.

815 [51] J. Tuckerman, G. Gonzalez, E. Sousa, X. Wan, J. Saito, M. Alam, M. Gilles-Gonzalez, An
816 oxygen-sensing diguanylate cyclase and phosphodiesterase couple for c-di-GMP control,
817 *Biochemistry* 48 (2009). 10.1021/bi901409g.

818 [52] M. Gilles-Gonzalez, E. Sousa, *Escherichia coli* DosC and DosP: a role of c-di-GMP in
819 compartmentalized sensing by degradosomes, *Advances in microbial physiology* 75 (2019).
820 10.1016/bs.ampbs.2019.05.002.

821 [53] E. Groisman, The pleiotropic two-component regulatory system PhoP-PhoQ, *Journal of*
822 *bacteriology* 183 (2001). 10.1128/JB.183.6.1835-1842.2001.

823 [54] M. Castelli, E. García Véscovi, F. Soncini, The phosphatase activity is the target for Mg²⁺
824 regulation of the sensor protein PhoQ in *Salmonella*, *The Journal of biological chemistry* 275
825 (2000). 10.1074/jbc.M909335199.

826 [55] E. Véscovi, Y. Ayala, E. Di Cera, E. Groisman, Characterization of the bacterial sensor
827 protein PhoQ. Evidence for distinct binding sites for Mg²⁺ and Ca²⁺, *The Journal of biological*
828 *chemistry* 272 (1997). 10.1074/jbc.272.3.1440.

829 [56] S. Dubrac, T. Msadek, Identification of genes controlled by the essential YycG/YycF two-
830 component system of *Staphylococcus aureus*, *Journal of bacteriology* 186 (2004).
831 10.1128/jb.186.4.1175-1181.2004.

832 [57] S. Dubrac, P. Bisicchia, K. Devine, T. Msadek, A matter of life and death: cell wall
833 homeostasis and the WalKR (YycGF) essential signal transduction pathway, *Molecular*
834 *microbiology* 70 (2008). 10.1111/j.1365-2958.2008.06483.x.

835 [58] M. Bush, T. Ghosh, M. Sawicka, I. Moal, P. Bates, R. Dixon, X. Zhang, The structural basis
836 for enhancer-dependent assembly and activation of the AAA transcriptional activator NorR,
837 *Molecular microbiology* 95 (2015). 10.1111/mmi.12844.

838 [59] B. Yang, X. Nie, Y. Xiao, Y. Gu, W. Jiang, C. Yang, Ferrous-Iron-Activated Transcriptional
839 Factor AdhR Regulates Redox Homeostasis in *Clostridium beijerinckii*, *Applied and*
840 *environmental microbiology* 86 (2020). 10.1128/AEM.02782-19.

841 [60] A. Fiévet, L. My, E. Cascales, M. Ansaldi, S. Pauleta, I. Moura, Z. Dermoun, C. Bernard, A.
842 Dolla, C. Aubert, The anaerobe-specific orange protein complex of *Desulfovibrio vulgaris*
843 *hildenborough* is encoded by two divergent operons coregulated by σ_{54} and a cognate
844 transcriptional regulator, *Journal of bacteriology* 193 (2011). 10.1128/JB.00044-11.

845 [61] A. Fiévet, E. Cascales, O. Valette, A. Dolla, C. Aubert, IHF is required for the transcriptional
846 regulation of the *Desulfovibrio vulgaris* Hildenborough *orp* operons, *PLoS One* 9 (2014)
847 e86507. 10.1371/journal.pone.0086507.

848 [62] M. Ortmayer, P. Lafite, B. Menon, T. Tralau, K. Fisher, L. Denkhaus, N. Scrutton, S. Rigby,
849 A. Munro, S. Hay, D. Leys, An oxidative N-demethylase reveals PAS transition from ubiquitous
850 sensor to enzyme, *Nature* 539 (2016). 10.1038/nature20159.

851 [63] E. Stuffle, M. Johnson, K. Watts, PAS domains in bacterial signal transduction, *Current*
852 *opinion in microbiology* 61 (2021). 10.1016/j.mib.2021.01.004.

853